THE ASTRONOMICAL JOURNAL VOLUME 73, NUMBER 7 SEPTEMBER 1968

Motions and Structure of the Filamentary Envelope of the Crab Nebula

VIRGINIA TRIMBLE*
Mount Wilson and Palomar Observatories, Carnegie Institution of Washington, California Institute of Technology

(Received 1 May 1968)

Proper motions have been measured for 132 line-emitting filaments in the Crab Nebula on direct plates taken with the 100- and 200-in. telescopes. These motions, if assumed constant and extrapolated backward in time, converge toward a point about 12″ southeast of the double star near the center of the nebula. The filaments approach, on the average, most closely to that point or expansion center in about the year 1140, indicating that the expansion has been somewhat accelerated. Proper motions and radial velocities were measured for an additional 126 features on the same direct plates and Mt. Wilson and Palomar spectra. These, along with other, nondynamical data, indicate a most probable distance to the object of 2.02 kpc. Two projections of the nebula perpendicular to the one seen in the plane of the sky are constructed and do not differ significantly from that presented to us. The proper motion and radial velocity of the nebula as a whole are found and converted into galactic coordinates. This requires several assumptions of questionable validity. The nebula seems to be moving about 114 km/sec faster than the galactic rotation at its position. The proper motion of the so-called central star translates into an equally unlikely space motion, but this is also extremely uncertain. The likelihood of a physical connection between the star and the nebula is discussed. The line-emitting filaments are shown to be distributed throughout the nebula rather than being confined to a thin outer envelope. The motions are largely radial, each filament having a velocity approximately proportional to its distance from the expansion center. The deviations from this proportionality are as large as 0.032″/yr or 300 km/sec and have mean values near 0.010″/yr or 70 km/sec. These deviations are correlated with the scatter of the filaments around the expansion center in 1140.

I. INTRODUCTION

THE Crab Nebula now occupies that part of the sky where the Chinese reported seeing a "guest star" or supernova in 1054 (Duyvendak 1942). It is the only historically well-documented supernova remnant readily accessible to study by optical methods. Despite its uniqueness and availability, its internal motions and structure have by no means been completely described. The present paper attempts such a description based upon newly obtained proper motions and radial velocities of that component of the nebula characterized by a filamentary structure and a line emission spectrum. The nebula also emits continuous radiation which is relatively featureless.

The filaments define quite accurately an ellipse in the plane of the sky, except for a bulge on the south preceding edge. The ellipse has its center about 4″.7 east of the north following component of the 15th magnitude double star near the center of the nebula (Baade 1942). The axes of the ellipse are about four and six minutes of arc in length, the major axis lying in position angle 133°28′.

The best proper motions previously published (Duncan 1939), representing just 20 features near the edges of the nebula, clearly reveal a radial expansion. These motions have been analyzed (Duncan 1939; Baade 1942; Brosche 1966) to determine the center of that expansion and its time scale. The distance to the object has also been derived from these motions and radial velocities. Considerable improvement in quantity and quality of proper motions and the resulting analysis is now possible.

Woltjer (1958) and Münch (1958) have published radial velocities for more than 100 positions in the nebula. These positions were not indicated with sufficient accuracy that a given velocity could be identified with any particular feature on a direct plate. Such identifications can now be made.

II. MATERIALS AND MEASURING TECHNIQUES

Six direct plates, as listed in Table I, all taken in the light of the Hα and [N II] emission lines, were measured for proper motions.

These plates have two advantages over the earlier 60″ plates used by Duncan. First, of course, the larger scale (16.00 ″/mm on the 100 in. and 11.14 ″/mm on the 200 in. plates) allows positions to be determined more accurately. Secondly, the isolation of these emission lines by the use of a color filter and red-sensitive plates reveals a vast number of sharp, discrete features or filaments Plate I. The earlier orthochromatic plates, taken without any filter, show primarily the featureless continuum emission. Only a few of the strongest filaments appear in the light of Hβ and *N*1 and *N*2.

TABLE I. Direct plates used in proper motion study.

Date	Telescope	Plate	Filter	Exposure	Observer	Filaments measured
1939	100 in.	*	RG2	178 min	Baade	1–259
1953	100 in.	103a-E	RG2	165	Baade	1–259
1966	100 in.	Ia-E	RG2	120	Münch	132–259
1950	200 in.	103a-E	RG2	45	Baade	1–259
1964	200 in.	103a-E	RG1	67	Münch	1–259
1966	200 in.	103a-E	Hα	70	Münch	132–259

* Ammoniated red-sensitive plate, approximately equivalent to modern 103a-E.

* National Science Foundation Fellow 1966–68.

TABLE II. Proper motions of filaments shown in Plate I.

Filament	x (sec of arc)	y (sec of arc)	μ_x (″/yr)	μ_y (″/yr)	μ_r (″/yr)	E_μ (%)	α (deg)	σ_α (deg)
1	+140.1	− 59.4	+.157	−.052	.166	2.1	108.2	1.0
2	+133.5	− 59.9	+.156	−.030	.159	2.1	100.8	1.8
3	+125.5	− 65.5	+.154	−.072	.170	4.9	115.2	0.5
4	+132.3	− 41.4	+.145	−.026	.148	0.5	100.2	4.5
5	+ 22.6	−112.4	+.018	−.123	.124	13.5	171.5	0.9
6	+ 96.4	+ 38.3	+.113	+.062	.130	6.8	51.1	0.8
7	+ 82.6	− 90.5	+.086	−.115	.146	3.5	142.7	7.8
8	+ 19.5	− 75.5	+.008	−.077	.078	11.1	174.1	2.8
9	− 31.2	− 85.5	−.018	−.083	.086	14.1	192.5	2.0
10	− 35.1	− 89.3	−.021	−.082	.086	19.4	193.0	7.2
11	− 84.1	− 49.4	−.106	−.051	.119	6.3	244.1	5.0
12	− 97.6	− 53.5	−.132	−.058	.144	2.7	246.2	1.9
13	− 94.8	− 47.9	−.132	−.042	.138	5.2	252.4	1.6
14	− 70.4	+ 93.4	−.105	+.122	.164	3.2	319.5	9.5
15	− 20.8	+129.7	−.009	+.178	.178	3.0	357.1	2.1
16	−110.8	+ 94.2	−.143	+.131	.194	2.0	312.4	1.7
17	−117.0	+ 89.0	−.158	+.142	.212	0.6	311.9	2.4
18	+110.9	+ 9.7	+.122	+.028	.126	6.0	75.7	2.0
19	+ 50.5	−110.4	+.057	−.114	.128	1.4	153.3	6.4
20	−106.2	+ 32.3	−.135	+.050	.145	4.2	290.6	3.1
21	+ 49.2	+119.3	+.036	+.155	.159	0.2	12.9	1.9
22	+ 48.8	+122.1	+.045	+.155	.162	8.1	16.3	1.2
23	+ 68.3	+ 80.5	+.069	+.125	.143	4.2	28.6	5.6
24	− 68.3	+109.3	−.089	+.130	.157	2.1	325.4	2.0
25	− 62.5	− 90.6	−.085	−.090	.124	0.0	223.5	0.0
26	− 85.8	−100.1	−.119	−.111	.163	0.4	226.9	1.7
27	−130.6	+ 46.3	−.174	+.056	.183	2.6	287.7	1.8
28	−108.3	+ 60.6	−.146	+.087	.170	6.3	300.9	2.6
29	−104.0	− 1.5	−.128	−.004	.128	21.3	267.2	4.0
30	− 95.9	− 24.8	−.132	−.010	.133	7.6	265.6	0.1
31	− 84.5	− 28.2	−.119	−.012	.121	4.6	264.1	6.8
32	+ 42.0	− 77.3	+.054	−.080	.096	4.5	145.8	6.0
33	+ 87.4	+ 67.3	+.118	+.115	.165	2.8	45.6	0.8
34	+ 12.0	+110.7	+.013	+.150	.151	1.0	4.9	3.0
35	− 7.0	+120.7	−.022	+.157	.159	15.0	352.7	4.2
36	+ 86.3	− 15.2	+.084	−.002	.084	17.2	92.0	2.8
37	− 85.8	+123.3	−.100	+.162	.191	7.6	327.9	3.2
38	+116.0	+ 8.1	+.166	+.027	.169	13.6	80.9	0.1
39	+126.0	+ 4.8	+.136	+.021	.133	8.1	80.7	1.6
40	+131.0	− 8.7	+.144	+.020	.146	4.3	82.3	6.8
41	+155.0	− 25.4	+.126	−.051	.136	29.3	113.7	5.1
42	+139.5	− 40.4	+.134	−.030	.138	7.5	102.7	2.1
43	+103.0	− 77.0	+.126	−.084	.154	6.3	124.4	9.1
44	+ 91.0	− 79.4	+.122	−.087	.150	1.1	125.3	1.3
45	+ 42.4	−133.0	+.025	−.148	.150	1.4	170.3	0.5
46	+ 18.7	−109.1	+.009	−.132	.132	8.2	176.0	0.8
47	− 10.1	− 80.1	−.017	−.083	.086	10.8	192.8	9.4
48	− 20.8	− 86.6	−.048	−.092	.104	1.2	207.4	4.3
49	− 35.1	−100.6	−.049	−.114	.124	13.2	203.1	1.6
50	− 64.7	− 97.5	−.079	−.106	.132	13.4	216.4	3.0
51	− 81.0	− 84.7	−.095	−.082	.126	19.0	230.4	5.8
52	−105.6	− 71.0	−.136	−.098	.169	0.5	234.1	5.1
53	− 86.6	− 70.8	−.113	−.072	.134	0.8	237.4	2.8
54	−105.0	− 59.8	−.138	−.066	.154	3.8	243.9	1.4
55	−116.9	− 28.2	−.140	−.026	.143	5.4	259.2	1.2
56	−118.7	− 5.7	−.138	−.028	.141	1.7	258.3	3.6
57	−132.9	+ 1.7	−.150	−.002	.150	17.6	269.2	1.2
58	−141.0	+ 11.3	−.212	+.020	.214	11.2	275.0	5.0
59	−145.0	+ 34.7	−.221	+.044	.225	5.3	281.1	0.1
60	−105.6	+ 70.7	−.153	+.085	.176	1.8	299.1	5.1
61	−144.6	+ 76.4	−.177	+.096	.202	11.1	298.4	0.9
62	−104.2	+ 91.0	−.132	+.132	.186	0.2	314.9	1.5
63	− 93.4	+109.3	−.118	+.139	.183	2.0	319.6	1.6
64	− 60.2	+112.2	−.080	+.147	.168	3.8	331.2	1.1
65	− 60.9	+122.4	−.056	+.158	.168	4.9	340.6	4.2
66	− 15.0	+ 98.2	−.032	+.118	.124	4.8	345.6	8.1
67	− 5.5	+105.7	−.019	+.138	.139	1.4	352.4	4.0
68	+ 19.5	+110.6	+.014	+.141	.142	3.0	6.0	3.0
69	+ 37.1	+ 93.2	+.038	+.137	.143	7.3	14.8	6.4
70	+ 49.8	+ 87.4	+.052	+.101	.115	15.3	28.1	4.5
71	+ 72.8	+ 76.2	+.061	+.105	.122	18.2	29.0	5.0
72	+ 82.9	+ 84.4	+.103	+.139	.173	6.6	36.7	0.9
73	+101.9	+ 69.0	+.115	+.084	.143	2.1	54.2	5.0
74	+ 99.2	+ 50.3	+.110	+.073	.133	2.9	56.6	5.3
75	+ 96.7	+ 29.1	+.112	+.043	.120	8.8	68.4	7.4
76	+ 45.1	− 29.6	+.050	−.032	.063	21.8	127.0	19.0
77	+ 62.3	− 24.2	+.062	−.009	.063	24.0	98.4	0.2
78	+ 71.7	− 22.4	+.076	−.003	.077	7.6	92.6	5.2
79	+ 54.8	− 47.6	+.041	−.042	.059	20.4	134.3	6.1
80	+ 74.4	− 38.1	+.062	−.013	.063	4.0	102.4	4.6
81	+103.5	− 33.0	+.087	−.016	.088	8.4	100.2	2.1
82	+ 30.8	− 8.9	+.032	−.001	.033	2.2	91.3	11.5
83	+ 44.7	− 2.0	+.046	+.016	.049	7.4	70.7	4.5
84	+ 62.5	+ 5.1	+.071	+.020	.074	3.4	74.4	0.3
85	+ 44.0	+ 15.5	+.047	+.037	.060	11.8	51.8	2.5
86	+ 51.8	+ 26.6	+.059	+.039	.071	24.4	56.8	1.0
87	+ 63.8	+ 41.7	+.070	+.059	.094	20.3	46.9	13.5
88	+ 27.1	+ 37.3	+.024	+.059	.064	1.2	21.7	0.5
89	+ 46.9	+ 52.3	+.054	+.088	.103	13.0	31.2	0.4
90	+ 39.6	+ 71.2	+.035	+.087	.094	2.6	22.1	4.2
91	+ 20.0	+ 49.1	+.013	+.063	.065	12.2	12.3	6.8
92	+ 37.0	+ 59.7	+.045	+.091	.102	0.1	26.3	1.8
93	+ 4.5	+ 59.6	−.015	+.080	.082	3.2	342.0	2.0
94	+ 16.3	+ 79.9	+.013	+.102	.103	6.1	7.6	2.6
95	− 5.5	+ 88.4	−.005	+.119	.119	1.1	2.3	2.8
96	− 32.9	+ 66.9	−.039	+.096	.105	4.6	337.8	4.8
97	− 33.1	+ 84.4	−.044	+.104	.114	3.9	337.1	1.9
98	− 50.2	+ 97.8	−.053	+.138	.148	0.1	339.1	2.5
99	− 51.0	+ 66.0	−.066	+.081	.105	6.6	320.7	0.9
100	− 72.9	+ 80.1	−.112	+.111	.158	2.5	315.0	1.2
101	− 76.2	+ 54.1	−.112	+.088	.143	3.2	308.0	3.5
102	− 85.5	+ 23.2	−.117	+.033	.122	1.4	285.6	1.4
103	− 64.0	+ 19.9	−.079	+.020	.083	13.2	282.6	10.1
104	− 69.1	+ 38.8	−.098	+.036	.105	2.9	290.1	4.5
105	− 50.6	+ 33.1	−.064	+.047	.080	33.2	303.2	8.8
106	− 32.2	+ 47.9	−.043	+.089	.101	10.4	333.1	12.2
107	− 23.2	+ 20.0	−.040	+.023	.053	22.7	299.8	21.9
108	− 85.8	− 0.8	−.116	+.003	.116	1.2	271.6	1.6
109	− 57.3	− 0.5	−.080	−.001	.080	0.8	269.3	2.1
110	− 20.1	− 23.0	−.042	−.013	.045	56.6	249.9	5.5
111	− 64.1	− 19.3	−.073	−.012	.074	0.8	260.9	1.5
112	− 59.0	− 36.9	−.098	−.007	.102	5.2	264.8	15.6
113	− 61.4	− 59.1	−.093	−.053	.108	3.0	240.7	1.6
114	− 42.6	− 45.9	−.045	−.040	.060	1.6	228.5	3.8
115	− 30.1	− 57.4	−.068	−.068	.097	3.4	224.9	5.3
116	− 9.2	− 57.5	−.015	−.069	.071	1.3	191.8	8.1
117	+ 18.7	− 43.5	−.004	−.039	.039	56.6	183.1	3.8
118	+ 84.5	− 64.0	+.106	−.056	.120	3.8	117.7	0.3
119	+156.0	− 56.4	+.172	−.062	.183	0.8	109.6	1.6
120	+146.8	− 4.6	+.127	+.017	.128	62.2	82.4	9.9
121	+120.5	+ 58.9	+.156	+.086	.180	4.8	60.7	8.6
122	+ 24.7	+134.1	+.015	+.073	.174	3.1	4.8	4.8
123	− 1.6	+133.3	+.003	+.160	.161	2.8	1.0	7.0
124	− 58.0	+143.6	−.070	+.184	.198	2.2	339.3	5.6
125	−110.0	+125.2	−.148	+.158	.217	1.1	317.0	1.2
126	−131.8	+ 90.2	−.160	+.104	.191	8.8	303.3	1.2
127	−151.8	+ 54.8	−.202	+.073	.215	14.8	290.3	3.6
128	− 24.1	−110.6	−.035	−.120	.125	1.8	196.3	1.8
129	+ 63.0	−141.4	+.038	−.156	.161	10.8	166.0	3.4
130	+112.8	−111.9	+.141	−.137	.198	4.9	134.5	5.9
131	+131.5	− 83.1	+.162	−.112	.167	2.7	125.7	2.1
132	− 32.9	− 15.9	−.052	−.015	.054	5.8	253.9	3.6

The filaments first measured for proper motion (Nos. 1–132 of Table II and Plate I) are more or less uniformly distributed over the surface of the nebula. They are all small, distinct, and readily identifiable on all six plates.

Each of the four earliest plates was measured in four orientations differing by 90°. Settings were made with cross hairs on the ground glass projection screen of a Grant measuring machine (described in Greenstein and Trimble 1967). The 200-in. plates were also measured with a conventional traveling microscope. The plates were oriented by aligning two stars (A and B of Plate I) on the cross hairs. Positions of 132 filaments and 35 reference stars were recorded with respect to

the axis through these stars (position angle 76°18′) and later rotated to right ascension and declination coordinates.

The measured positions were reduced using the method of dependences (van de Kamp 1962). This was done twice. Each filament was compared first with the four stars closest to it and then with all the stars (except the south preceding component of the central double star, E in Plate I, which has considerable proper motion). The results from the two measuring engines and the two methods of reduction do not differ by more than the inaccuracy of a single setting (2 to 5 μ, depending on the size and shape of the feature involved). Quite by chance, the scales and time separations of the plates are such that a 1-μ difference in position between the 1939 and 1953 or the 1950 and 1964 plates corresponds to about 0.001″/yr of proper motion. The tabulated values are those obtained from the Grant machine and the reduction using all the stars.

Twenty-four spectra from the Mt. Wilson and Palomar Observatories plate collection were measured for radial velocities. The 18 spectra by Münch include those previously published (Münch 1958). Most of these were taken with the nebular spectrographs of the 100-in. and 200-in. telescopes. The 300-groove/mm grating used is blazed in the third order at Hα and gives dispersions of 110 or 215 Å/mm, depending on the focal length of the camera. A few other plates, taken with a different grating, have dispersions near 400 Å/mm. Table III lists the lines measured.

Six plates at 215 Å/mm taken by Minkowski were also measured. These have the third, fourth, and fifth orders overlapped (but only a third-order comparison spectrum) and, therefore, show many more lines. Only [N II] and Hα were measured.

All spectra were measured using the oscilloscope of the Grant measuring machine. A single spectrum (Plate II) shows from three to thirty separate features. The streaks perpendicular to the slit directions are stars. Two or more features overlap in many cases (for example, point X in Plate II). This overlapping reduces the accuracy with which the positions of the lines can be determined. Fortunately the spacing of the emission lines is such that if the [S II] lines of two features are blended, the [N II] and Hα lines are not, and vice versa. Where there is no blending, settings on the Grant machine are usually repeatable to within 1 μ (5 to 20 km/sec at the dispersions involved). The standard deviations of velocities determined from several lines are generally in this range.

Curvature of the spectral lines perpendicular to the direction of disperison is the other main source of error. The apparent difference in velocity between two positions along the slit due to this curvature can easily be calculated for a perfect optical system (Minkowski 1942a). It should depend only on the distances of the two positions from the center of the slit and on the focal length of the camera.

TABLE III. Emission lines measured in spectra of Crab Nebula.

Wavelength	Element	Intensity
6730.48	[S II]	Medium
6716.42	[S II]	Medium
6583.37	[N II]	Strong
6562.82	H	Strong
6548.06	[N II]	Strong
6300.27	[O I]	Faint, often absent

As a check on the calculated values, empirical curvature corrections were determined from several calibration plates having comparison lines along the full length of the slit. These plates were taken at the same time and with the same optical setups as the various spectra. Pairs of such plates taken with the same camera and grating on the same telescope were not entirely in agreement, and the curvature correction was found to be a function of wavelength. This may reflect a dependence on distance from the optical axis of the system. On the widest 200-in. telescope spectra, for example, the calculated velocity shift between the center of the spectrum and the point where the comparison lines were measured was 103 km/sec. The observed shift on one calibration plate ranged from 71 km/sec at the [S II] lines to 114 km/sec at the [O I] line, while another plate taken the same year with the same optical setup showed a range of 77 to 154 km/sec over the same wavelength region.

The velocities from each spectrum of the nebula were corrected in accordance with the calibration plate taken with the same camera and grating at most nearly the same time. The resulting error may be as great as 15 km/sec for the velocities of a few filaments furtherest from the comparison lines. In most cases, it is less than 10 km/sec.

About 25 features appear on two or more (parallel or intersecting) spectra. Where this occurs, the several velocities for a single filament differ by less than their probable errors. The velocity tabulated for such a filament is the average of the values from the various plates.

Positions of the features along the slit (with respect to stars on plates where they occur, otherwise with respect to the center of the slit) were recorded at the time the spectra were measured. Using these positions, the spectra were compared with direct plates. Because Münch's original observing charts were still available, velocities could be associated with particular features on the direct plates for all but two of the spectra. It became possible to do this for Minkowski's spectra only after the proper motion measurements had been completed.

The 127 features with known radial velocities found in this way (Nos. 133–259 of Table IV and Fig. 1) were then measured with the Grant machine on all six direct plates. These were reduced in the same fashion as the first set of proper motion measurements for the

TABLE IV. Proper motions and radial velocities of filaments shown in Fig. 1.

Filament	x (sec of arc)	y (sec of arc)	μ_x (″/yr)	μ_y (″/yr)	V_r (km/sec)	σ_v (km/sec)
133	− 31.1	+ 89.8	−.035	+.105	+ 56	7
134	− 46.9	+ 98.4	−.066	+.125	+ 130	14
135	− 37.1	+ 94.6	−.051	+.126	+ 113	16
136	− 55.7	+100.9	−.077	+.123	+ 125	...
137	− 7.1	+ 65.4	−.018	+.095	− 311	11
138	− 11.7	+ 61.3	−.019	+.081	− 527	4
139	− 19.3	+ 54.6	−.030	+.065	− 662	6
140	− 31.4	+ 35.8	−.039	+.042	+1382	...
141	− 23.6	+ 37.1	−.027	+.055	− 719	20
142	− 45.9	+ 25.6	−.064	+.026	− 932	20
143	− 45.3	+ 20.3	−.062	+.033	− 918	...
144	− 66.4	+ 6.5	−.098	+.012	− 439	24
145	+ 1.4	+ 49.4	−.012	+.062	+ 874	28
146	+ 86.8	+ 44.3	+.088	+.063	− 84	...
147	+ 94.1	+ 35.9	+.110	+.054	− 274	28
148	+ 97.3	+ 28.2	+.106	+.046	− 234	...
149	+ 94.1	+ 13.7	+.102	+.030	− 601	...
150	+ 95.8	+ 11.3	+.095	+.064	− 672	...
151	+103.5	− 32.5	+.096	−.025	+ 844	33
152	+ 89.0	+ 40.8	+.114	+.055	− 808	5
153	+ 96.2	+ 38.1	+.113	+.059	+ 18	1
154	+ 99.3	+ 35.9	+.117	+.060	+ 498	36
155	+101.9	+ 30.2	+.127	+.054	+ 39	5
156	+105.9	+ 19.9	+.125	+.042	− 550	6
157	− 19.2	− 0.3	−.032	+.014	− 698	46
158	− 9.4	− 0.9	−.013	−.001	+ 89	0.1
159	− 2.9	− 0.4	−.003	+.000	− 162	50
160	+ 4.6	+ 0.8	−.007	+.002	− 369	16
161	+ 57.2	− 1.2	+.054	+.009	+ 950	13
162	+ 26.7	+ 92.1	+.026	+.117	+ 631	102
163	+ 12.3	+ 92.1	+.013	+.117	− 304	30
164	− 3.6	+ 91.7	−.005	+.122	+ 130	42
165	− 13.8	+ 89.5	−.027	+.133	+.102	7
166	− 28.0	+ 88.4	−.038	+.104	+ 119	25
167	− 23.0	+ 88.6	−.032	+.128	− 455	8
168	− 54.1	+ 88.3	−.075	+.118	− 350	...
169	− 65.1	+ 84.4	−.093	+.110	− 962	...
170	+ 55.0	+ 78.0	+.047	+.095	− 145	34
171	+ 48.5	+ 47.5	+.043	+.067	+ 340	6
172	+ 41.4	+ 13.1	+.032	+.013	+ 484	3
173	+ 43.1	+ 11.3	+.046	+.013	+ 548	24
174	+ 44.6	− 2.0	+.042	+.010	− 293	...
175	+ 37.8	+ 2.7	+.044	+.020	− 882	...
176	+ 33.7	− 31.3	+.037	−.012	+ 683	13
177	+ 30.2	− 54.8	+.020	−.057	+ 439	9
178	+ 30.2	− 71.0	+.031	−.102	+ 80	16
179	+ 24.4	− 78.4	+.018	−.107	+ 557	32
180	−126.5	− 94.6	−.153	−.150	− 879	2
181	−107.0	−100.9	−.122	−.135	− 732	8
182	− 86.6	−100.6	−.098	−.122	− 217	50
183	− 76.3	+ 0.0	−.102	+.003	− 376	14
184	− 68.7	− 0.6	−.101	−.006	− 313	14
185	− 87.1	+ 11.1	−.119	+.010	− 198	10
186	− 93.2	+ 17.5	−.126	+.022	− 142	14
187	− 85.9	− 0.9	−.121	−.002	− 698	...
188	−106.4	+ 22.6	−.126	+.033	− 798	...
189	−112.9	+ 25.5	−.162	+.033	− 960	...
190	−121.0	+ 29.9	−.148	+.046	+ 716	9
191	−138.7	+ 40.7	−.185	+.060	+ 444	...
192	−147.9	+ 49.6	−.188	+.063	+ 356	...
193	+ 26.4	− 61.3	+.022	−.064	+ 463	19
194	− 23.6	− 30.0	−.039	−.023	+ 797	19
195	− 29.6	− 22.6	−.051	−.018	+ 682	8
196	− 31.7	− 22.1	−.064	−.013	+ 544	8
197	− 27.8	− 29.3	−.051	−.028	− 665	1
198	− 35.6	− 27.8	−.064	−.018	− 544	13
199	− 38.2	− 26.1	−.063	−.026	− 432	4
200	− 47.5	− 18.3	−.082	−.017	− 408	7
201	− 65.4	− 9.0	−.095	−.000	− 403	16
202	− 79.3	+ 1.4	−.095	+.010	− 316	5
203	− 31.9	− 29.5	−.053	−.021	− 596	18
204	− 35.7	− 20.1	−.058	−.015	− 487	17
205	− 83.4	+ 6.6	−.097	+.013	− 232	13
206	+ 52.6	+ 6.6	+.051	+.023	+ 404	24
207	+ 30.4	− 0.7	+.022	+.014	− 777	18
208	+ 17.9	− 4.2	+.008	+.016	− 733	7
209	+ 25.5	− 7.9	+.018	+.010	+ 682	13
210	− 84.0	− 49.6	−.114	−.049	+ 210	36
211	+ 8.0	+ 58.0	+.000	+.084	+ 598	16
212	+ 15.6	+ 63.7	+.006	+.085	+ 871	...
213	+ 16.9	+ 70.1	+.005	+.095	− 738	8
214	+ 18.3	+ 62.3	+.011	+.084	− 823	10
215	+ 9.2	+ 62.2	+.002	+.086	− 889	11
216	+ 5.7	+ 54.5	+.011	+.086	+ 782	12
217	+ 7.4	+ 46.2	−.006	+.054	−1122	...
218	− 10.7	+ 25.5	−.029	+.044	+1299	...
219	− 11.9	+ 19.6	−.027	+.037	+1140	15
220	− 21.1	+ 7.8	−.033	+.009	−1482	44
221	− 28.1	− 3.2	−.038	−.001	−1385	21
222	− 30.7	+ 0.7	−.043	+.010	+1086	37
223	− 28.2	− 8.3	−.048	+.010	− 919	10
224	− 30.0	− 12.6	−.055	−.001	− 451	...
225	− 37.0	− 8.4	−.061	+.007	+ 920	27
226	− 36.8	− 12.0	−.065	+.004	− 566	22
227	− 38.4	− 23.7	−.070	+.013	− 448	18
228	+ 62.3	+ 75.9	+.060	+.111	− 179	11
229	+ 53.9	+ 68.4	+.052	+.079	+ 378	...
230	+ 45.8	+ 67.4	+.037	+.098	+ 522	...
231	+ 43.3	+ 62.3	+.036	+.073	+ 550	...
232	+ 38.0	+ 62.2	+.022	+.078	+ 500	3
233	+ 49.4	+ 72.9	+.048	+.097	− 62	...
234	+ 44.6	+ 70.2	+.042	+.099	− 155	21
235	+ 40.0	+ 68.1	+.032	+.091	− 297	36
236	+ 35.8	+ 69.4	+.017	+.095	− 327	30
237	+ 31.8	+ 60.9	+.022	+.082	− 536	25
238	+ 21.8	+ 63.5	+.001	+.081	− 561	29
239	− 5.3	+ 50.1	−.010	+.071	+1313	...
240	− 9.6	+ 50.7	−.015	+.071	+1144	15
241	− 25.3	+ 43.1	−.034	+.064	+ 982	30
242	− 30.8	+ 45.2	−.048	+.063	+ 850	16
243	− 12.8	+ 53.6	−.029	+.070	− 336	10
244	− 27.9	+ 43.6	−.031	+.064	− 591	12
245	− 32.3	+ 48.1	−.042	+.071	− 749	5
246	− 36.7	+ 41.1	−.067	+.063	+1647	...
247	− 62.2	+ 35.1	−.101	+.047	+1470	...
248	− 44.4	+ 44.0	−.065	+.055	−1026	...
249	− 61.5	+ 39.4	−.083	+.052	− 948	2
250	− 68.9	+ 33.6	−.095	+.043	− 980	...
251	− 78.8	+ 33.4	−.106	+.047	+ 964	0.4
252	− 90.1	+ 29.5	−.123	+.036	+1135	4
253	+ 39.5	+ 71.1	+.043	+.098	− 379	85
254	+ 32.6	+ 66.9	+.023	+.094	− 502	20
255	+ 43.5	+ 48.6	+.049	+.068	+ 264	12
256	+ 35.4	+ 55.5	+.041	+.073	− 365	5
257	+ 11.9	+ 69.7	+.010	+.091	+ 473	12
258	+ 3.7	+ 75.3	−.018	+.091	+ 199	13
259	− 16.2	+ 80.9	−.023	+.097	− 609	26

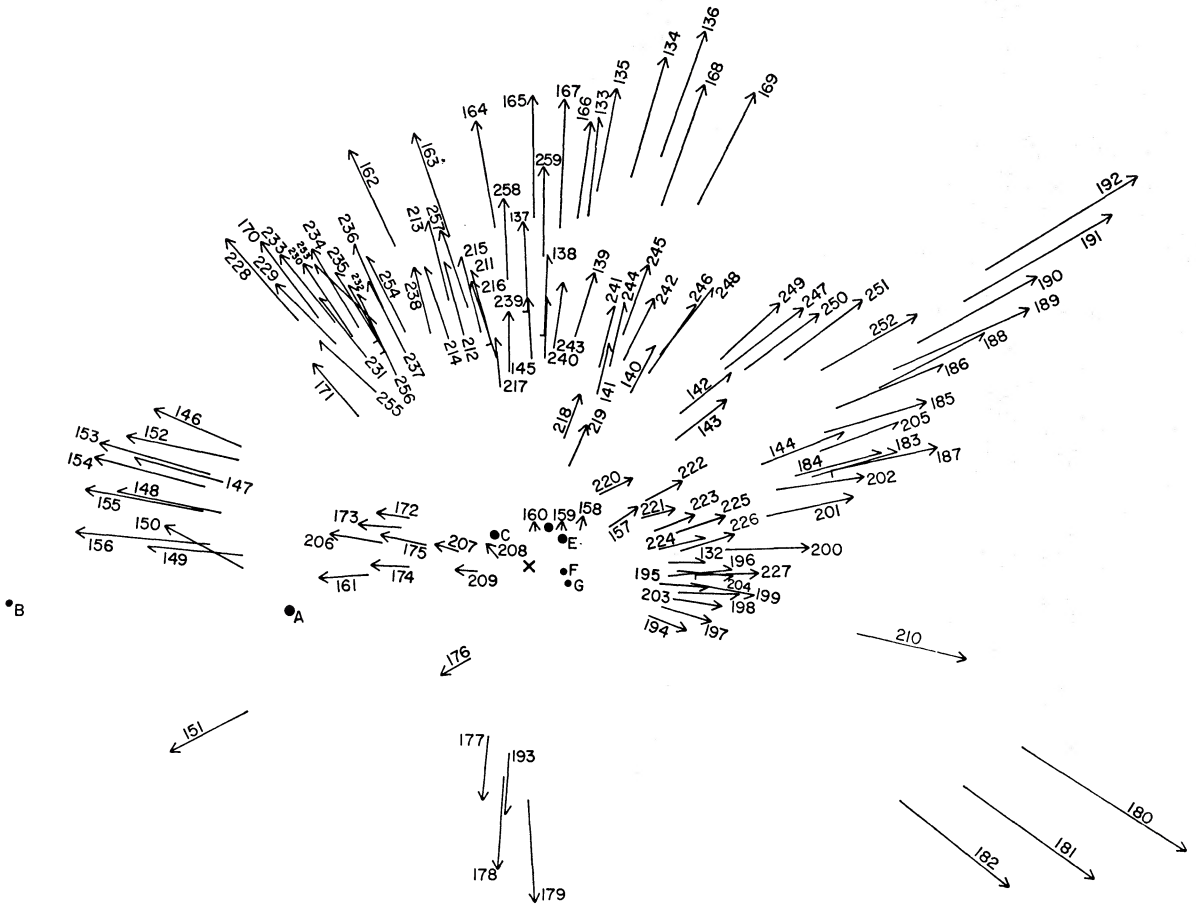

FIG. 1. Proper motions for the 127 filaments of known radial velocities as listed in Table IV. The scale and orientation are about the same as in Plate I, and X again marks the expansion center. The stars lettered in Plate I are also shown.

five pairs of plates 1939–1953, 1939-1966, 1953-1966 (100 in.) and 1950-1964 and 1950-1966 (200 in.). A proper motion in Table IV is the mean of the resulting five numbers. Since these features could not be chosen for ease of measurement on the direct plates, a single setting may be in error by 4 to 8 μ. These filaments are also much less uniformly distributed over the nebula than was the first set of features.

III. RESULTS

A. Proper Motions

Plate I shows the first set of filaments for which proper motions were determined. Many of the fainter features have been lost in the reproduction process, but they are easily seen and measured on the original plates. The arrows show the distance each filament will cover in about 270 yr at its present rate of motion. Table II lists the coordinates, x and y (for 1950), and proper motions, μ_x and μ_y, of the filaments identified in Plate I. Following Duncan (1939), these are given in seconds of arc in a rectangular coordinate system that corresponds to right ascension and declination near the center of the nebula. The origin is the north following component of the central double star (D in Plate I). The tabulated proper motions are the averages of the results from the two pairs of plates. These motions and all those tabulated and discussed below are relative to the group of 35 reference stars. The motions found for these stars are given in the Appendix.

The table also gives the total proper motion vector μ_r and its position angle α for each filament. The percentage error of the length E_μ is one-half the difference of the 100-in. and 200-in. results expressed as a percent of their average. This is less than 4.5% for

TABLE V. Expansion centers and dates of convergence of Crab Nebula.

Center	Plates	Reduction method	Right ascension of center	Declination of center	Date of best convergence
C1	100 in.	weighted mean	+6".3	−10".3	1131
C2	100 in.	least squares	+5".6	− 8".7	1134
C3	200 in.	weighted mean	+9".1	− 8".7	1147
C4	200 in.	least squares	+9".4	− 6".3	1149
Average			7".6±1".3	−8".5±1".1	

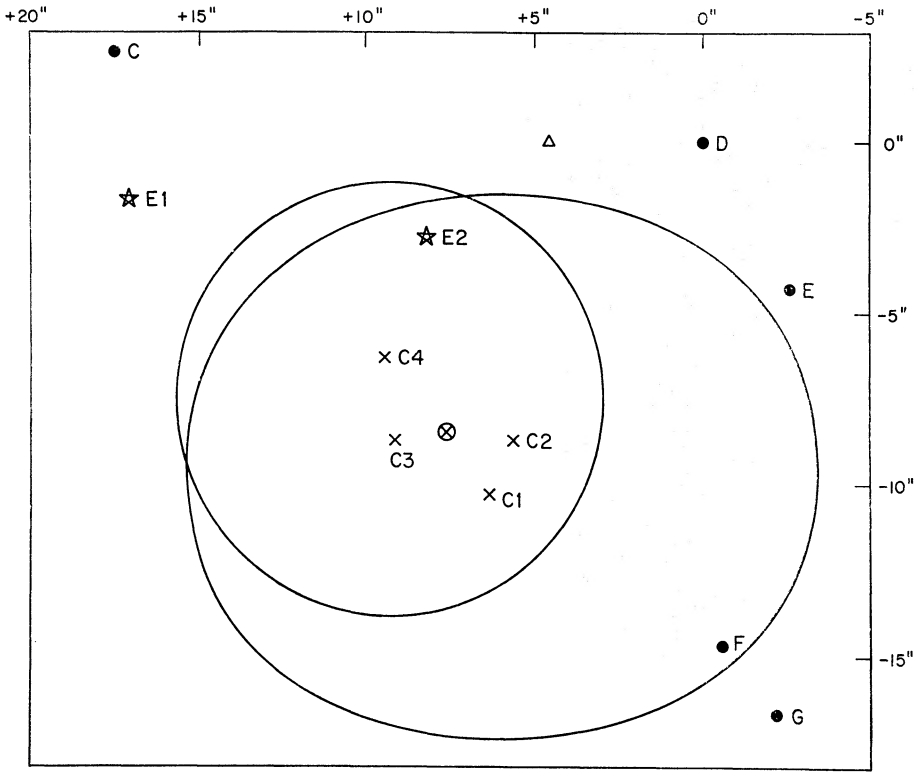

FIG. 2. Central region of the Crab Nebula showing the expansion centers listed in Table V (C1—C4 and their average) and the regions in which the filaments are concentrated at the time of best convergence. The present geometrical center of the nebula is shown as Δ. E1 and E2 are the 1054 positions of star E for proper motions of 0.019″/yr and 0.009″/yr, respectively.

one-half of the filaments and less than 11% for three-quarters of them. The probable error of the angle σ_α is one-half the difference of the 100-in. and 200-in. results. This is less than 3° for one-half of the filaments and less than 5° for three-quarters of them. There is no systematic difference in the angles determined from the two sets of data, but the 200-in. motions are, on the average, 3% larger than the 100-in. ones.

The sets of data from the two pairs of plates were analyzed separately to determine the center of expansion and the time when the filaments were, on the average, closest to that center. This was done in two ways. In the first case, the center was taken to be a weighted mean of the 8712 positions of the intersections of all possible pairs of proper motion vectors. The weight given to each point was the reciprocal of the distance that point is moved by a small change in one of the two motions involved. (This depends both on the lengths of the vectors and on the size of the angle between them.) The time was then found when the filaments were closest to that center, if their velocities have been constant.

In the second case, the center was taken to be that point to which all the filaments approached most closely (in a least-squares sense) at a single time. That time was also determined. It can be easily shown (by using, for example, three vectors that form a scalene triangle) that these two methods need not give the same answer.

Table V lists the results of these various operations. The coordinates again follow Duncan's convention. The positions found for the center are shown as C1, C2, C3, and C4 in Fig. 2 along with the five stars near the center of the nebula (C through G of Plate I). All of the centers (which are located about 12 sec of arc southeast of the north following star, D) fall within less than 6″ of one another.

The convergence of the filaments at the dates indicated is quite good. One-half of the filaments fall within a circle of radius 6″.4 around the center according to the 200-in. data. The corresponding area for the 100-in. data is an ellipse 8.1×9″.5. These areas are shown in Fig. 2.

The date of best convergence is about A.D. 1140—that is, somewhat earlier than Duncan found, but still far from 1054. The 16-yr difference between the two sets of data indicates that the error of the measurements is probably much less than this 90 or so years. Since convergence occurs later than 1054, evidently the present proper motions are larger than the average proper motions over the lifetime of the nebula. This could be accounted for by a gradual uniform acceleration. More or less random or pulsationlike variations about some mean velocity of expansion are also possible. If the 16-yr difference between the 100-in. and 200-in. results is real, it would tend to indicate a gradual acceleration, since the more recent pair of plates shows the larger velocities. Comparison of any of the dates

with Duncan's results (A.D. 1172, found from a 1909–1938 baseline) indicates quite the opposite. The 3% apparent increase in average motion mentioned above is, in any case, much too large to be interpreted as part of an approximately uniform acceleration since it occurs in only 11 yr.

Convergence dates were also found for the filaments lying near the major and minor axes of the nebula separately. These do not differ to within the accuracy of the determination (25 or so years, since fewer filaments are involved). This negative result indicates only that the nebula has expanded out of a very small area, as has already been shown. If the dates had differed systematically, in the sense of the major axis date being earlier than the minor axis date, it would have indicated either that the velocity field was established at a time when the nebula was already reasonably large and elliptical in shape or that the rate of acceleration along the minor axis has been smaller than along the major axis. A later major axis date would have indicated greater acceleration along the minor axis direction.

The proper motion of the nebula as a whole ought to be given by (present position of the center of mass −position of expansion center)÷age. The geometrical center of the ellipse (in the plane of the sky) filled by the faintest filaments is easily found. It is (Baade 1942) $4''.7\pm3''$ east and $0''.0\pm3''$ north of the north following star. There is, however, no particular reason to suppose that this coincides with the center of mass. Indeed, the concentration of both bright filaments and the brightest continuum emission on one side of the geometrical center indicates strongly that they do not coincide. In addition, both the radio emission at various frequencies and the x-ray emission from the nebula appear to have their centers northwest of the optical center (Matveenko and Sorochenko 1968; Bowyer *et al.* 1964; Oda *et al.* 1967). The small low-frequency radio source, on the other hand, is about 10″ southwest of the optical center (Gower 1967). Most of the activity observed in the continuum emission (discussed by Scargle 1968) is also on the northwest side of the geometrical center. Although some of that activity takes the form of outward moving, slightly curved wisps, their center is not sufficiently well determined to differentiate between the various other centers.

In addition, the assumption that the mass and geometrical centers are coincident yields an extremely unlikely value for the space motion of the nebula. This point is considered again after a discussion of the distance to the Crab Nebula, since this distance determines just how unlikely the resulting space motion will be.

Any attempt to find the over-all proper motion by analysis of the motions of individual filaments is also frustrated by this uncertainty of the center of mass coordinates.

Six of the stars measured have detectable proper motion (see the Appendix). One of these is the south preceding component of the central double star. Previously published values for its motion are seriously discordant. Duncan (1939) and Deutsch and Lavdovsky (1940) find $\mu_\alpha=-0.019''$/yr and $-0.018''$/yr, respectively, and μ_δ very nearly zero. Baade (1942) and van Maanen (1928) find $\mu_\alpha=-0.009''$/yr and $-0.007''$/yr, respectively, and confirm μ_δ near zero. The present measurements of all six direct plates give $\mu_\alpha=-0.009''$/yr with a probable error of $0.003''$/yr and $\mu_\delta=-0.002''$/yr with a similar probable error. Figure 2 shows the positions of the south preceding star in 1054, for both the larger and the smaller proper motion, as E1 and E2. This position is just the 1950 position minus $\mu\times(1950-1054)$. Baade, in calculating the position of this star at the time of the supernova explosion, made the curious assumption that the number of years entering into the sum should be (present date−1172) as though the star's motion had participated in the apparent acceleration of the nebular expansion. This seems to be totally unwarranted.

Neither proper motion brings the star's 1054 position within the region where the expansion center of the nebula most probably lies, but the coincidence is much closer than with Duncan's expansion center, which, on the scale of Fig. 2, lies a bit off the left side of the page at about the height of star C. The positions found for the star and nebula are not quite so near as might be expected if they are the remains of a single event, but the close approach is nevertheless suggestive, particularly since none of the other stars near the center of the nebula has a detectable proper motion.

Although there are no known spectra of stars which are remnants of supernovae anywhere near as old as the Crab Nebula, it might be expected that, if this star is physically connected with the nebula, it ought to be unusual in some way or other. Unfortunately it is not an easy star to observe because of the strong continuous emission of the surrounding nebula. Two spectra of the star have been taken at the Mt. Wilson and Palomar Observatories. The earlier one, taken by Minkowski (1942b), has no detectable lines. The more recent spectrum, taken by Kraft (1967), is somewhat underexposed, but appears to show weak lines of hydrogen and ionized calcium in absorption. Both of these spectra probably have a large and perhaps predominant component due to the nebular emission. If the star is, as the Kraft spectrum indicates, not very peculiar, then the probability of its being related to the nebula is greatly decreased. There are, after all, six stars very near the center of the nebula (C through G of Plate I and a 21st magnitude star between E and F).

B. Distance to the Crab Nebula

Before the proper motion and radial velocity data in Table IV can be combined to give a three-dimen-

sional picture of the Crab Nebula, its distance must be known. The dynamical data themselves suggest a range of probable distances within which a choice must be made on the basis of other considerations.

If the nebula were a uniformly expanding sphere or spherical shell, then the distance D might be found by setting the maximum observed radial velocity $V_r^{\max}$ (which ought to occur at the center of the nebula) equal to the maximum observed proper motion $\mu^{\max}$ (which should occur at the edges) in the formula

$$V_r^{\max} = 4.74 \mu^{\max} D, \quad (1)$$

where D is in parsecs, $V_r^{\max}$ in km/sec, and $\mu^{\max}$ in (sec of arc)/yr. Unfortunately, the object is, at best, some sort of an ellipsoid, and the blind use of formula (1) clearly implies the assumption that the axis of the ellipsoid along the line of sight is the same length as the major axis of the ellipse in the plane of the sky. An equally reasonable assumption might be that the axis along the line of sight is the same length as the minor axis in the plane of the sky. Anything in between or somewhat outside of this range is also, of course, possible. Distances have been calculated for only these two simple assumptions out of prejudice in favor of symmetry.

The largest measured radial velocities (filaments 220, 221, 246, and 247 of Table IV) seem, with some regard to their probable errors, to indicate a maximum of about 1450 km/sec. The largest velocities measured on Minkowski's plates, -1446 ± 18 km/sec and $+1482 \pm 41$ km/sec, confirm this.

The largest proper motions along the major axis are all about 0.222″/yr (filaments 58, 59, 125, and 127 of Table II). The procedure used by Baade to correct Duncan's proper motions to what they might have been if the features measured had been at the extreme ends of the major axis is in this case both unnecessary (since the filaments are very nearly there already) and unwise (since it assumes an absolutely uniform expansion). Any number in the range 0.220 to 0.225″/yr would be equally consistent with the data, but the value chosen has the particular virtue that 0.222″/yr × 810 yr = 180″, the length of the major axis.

Along the minor axis an unexpected difficulty arises. Some of the motions are much too large. Since the axial ratio of the ellipse in the plane of the sky is very nearly $\frac{2}{3}$, the largest proper motions near the ends of the minor axis ought to be about $\frac{2}{3} \times 0.222$″/yr or 0.148″/yr. There are, in fact, filaments (21, 22, 23, and 73 of Plate I and Table II) fulfilling this expectation ($\bar{\mu} = 0.151$″/yr). There are, however, other features near the minor axis having larger velocities. A couple of these (26 and 52) are located in the "bulge" that extends outside the otherwise well-defined ellipse on its south preceding edge. Their larger proper motion (about 0.163″/yr) is, therefore, not disturbing. Other filaments (33, 72, 121, and 122), however, lying near the minor axis but not in the bulge have proper motions near 0.171″/yr.

Filaments with motions smaller than the values listed also occur near the ends of both axes. These are of the order of 0.140″/yr near the end of the minor axis and 0.200″/yr for the major axis. Alternatively, therefore, the largest minor axis proper motions might have been taken as "normal" and the absence of major axis motions as large as 0.258″/yr ($\frac{3}{2} \times .172$″/yr) be regarded as surprising. Since the smaller motions have, at least, the virtue of actually occurring somewhere near the edges of the nebula, they will be used.

Returning to formula (1) and inserting $V_r^{\max} = 1450$ km/sec and $\mu^{\max} = 0.222$ or 0.151″/yr reveal that the Crab Nebula can be either an oblate spheroid at a distance of 1.38 kpc or a prolate spheroid at a distance of 2.02 kpc (or, in principle, any other consistent combination). The uncertainty of these numbers is rather great. If the largest and smallest possible values of proper motion and radial velocity indicated by the discussion above are put into formula (1), the distance for the oblate spheroid is found to range from 1.15 to 1.61 kpc and that of the prolate spheroid from 1.76 to 2.26 kpc.

The only other "distance" that can be found from the data of Table IV is the one that comes from assuming that all the filaments ought to have, as nearly as possible, the same total speed. This would be precisely true for a uniformly expanding thin spherical shell. Applying the assumption to the Crab Nebula gives a distance of 2.17 kpc, not very different from that just found for a prolate spheroid.

Because the positions of the filaments along the line of sight are not known, no estimate of the distance can be derived by requiring the filaments to come as close as possible to a single point (in three dimensions) at a single time, or from any similar consideration.

A number of independent, nondynamical arguments favor a distance around 2 kpc. Woltjer (1958) points out that a quantity involving the line ratio $[\text{O III}]_{N1+N2}/[\text{O II}]_{\lambda 3727}$, which ought to depend only on electron density, becomes nearly constant over the nebula only if this larger distance is assumed. If the smaller distance is correct, then the quantity depends strongly on the distance of an emitting filament from the center of the nebula.

Münch (1958) suggests that, since the direction of the major axis of the ellipse enclosing the filaments is very nearly the direction of the galactic equator at that point in the sky, the shape of the nebula might have been influenced by the interstellar magnetic field, the matter expanding most rapidly along lines of force (assumed parallel to the galactic equator). Both the minor axis direction and the line of sight are perpendicular to these lines of force, and the axes in these directions ought to be roughly equal and smaller than the major axis.

Minkowski (1964) favors the larger distance as bringing the maximum brightness of the observed supernova (deduced from the Chinese records) closer to the average of Type I events in other galaxies. The frequency of supernovae in our galaxy is also more like that found for the Virgo cluster if the larger of two possible distances is assumed for the Crab Nebula as well as for Tycho's and Kepler's supernovae. If, as has recently been suggested (Minkowski 1966), the supernova of 1054 was not a Type I event, this argument ceases to be relevant. His only counterargument is the large mass of the filaments implied by the larger distance. Shklovskii (1966) points out that the prolate shape associated with the larger distance is in better agreement with what is known about the ejection of matter from novae and explosions in galactic nuclei than is the oblate shape implied by a distance around 1 kpc. In addition, the interstellar absorption expected out to 2 kpc or so is sufficient that the continuous emission from the nebula can then be interpreted as synchrotron radiation with a constant spectral index over the entire frequency range 10^{12}–3×10^{16} cps. If the smaller distance is assumed, the spectral index must vary with frequency. He also notes that the mass of the filaments implied by the larger distance need not be intolerably large.

The two arguments dealing with the way in which the nebular matter was ejected tend also to favor the assumption of axial symmetry made above. The ensuing discussion, therefore, supposes that the Crab Nebula is 2.02 kpc from us.

C. Three-Dimensional Considerations

Table IV gives the positions, proper motions, and radial velocities of the 127 filaments identified in Fig. 1.

The radial velocities of individual filaments reveal the same sort of nonuniformity that was noted in the case of the proper motions. Just as the proper motions do not reach a unique maximum value at the edge of the nebula, the radial velocities do not tend to zero there; nor are the largest velocities found precisely at the center of the nebula. It is, therefore, only approximately true that the velocity of each filament is proportional to its distance from the expansion center. The fact that all filaments do converge to such a center at a single time shows that there is, in general, such a proportionality.

The resulting uncertainty in positions of filaments along the line of sight can be estimated. Proper motions at the extreme ends of the minor axis in the plane of the sky vary from 0.140 to 0.172″/yr, a range of 0.032″/yr, and radial velocities as large as 300 km/sec are found very near the edges of the nebula. Formula (1) shows that, for a distance of 2020 pc, these two numbers represent very nearly the same space motions. A filament of known radial velocity will, therefore, have a 1950 position along the line of sight given by its velocity times the age of the nebula (2.5×10^{10} sec), but that position will be uncertain by about 7×10^{12} km, or, in unreasonable units, 25 sec of arc projected to a distance of 2020 pc. This is about the distance, in the plane of the sky, from star C to star G, or a bit more than one-tenth of the minor axis. Subject to this limitation on accuracy, cross sections of the nebula perpendicular to the one shown in Fig. 1 can be constructed.

Figure 3 shows the positions and motions in 270 yr of filaments 133–259 in the major axis–line of sight cross section. Figure 4 represents the minor axis–line of sight cross section similarly. The side of the nebula toward us is at the bottom of Fig. 3 and to the left in Fig. 4. Both these cross sections appear rather circular. This is expected in the case of Fig. 4. In Fig. 3 it is a result of the total absence of filaments of known radial velocity anywhere near the ends of the major axis. The nonuniform distribution of the features over the nebula is also evident. When this nonuniformity is taken into account, these cross sections do not appear to differ significantly from the one presented to us in the plane of the sky. In particular, the stronger connected features visible on a direct plate can be readily traced in all three cross sections. It is interesting to note that the strongest of these are often the result of the superposition of two emitting regions on opposite sides (from our point of view) of the nebula.

If the assumption that the present geometrical center of the nebula coincides with its center of mass is correct, then the object as a whole has a proper motion (given by present center position minus expansion center position divided by age) $\mu_\alpha=-0.0036''$/yr and $\mu_\delta=+.0105''$/yr, or a total of 0.0111″/yr in position angle 341°4′. (This should be compared with the proper motion of the so-called central star, $\mu_\alpha=-0.009''$/yr, $\mu_\delta=-0.002''$/yr.) For a distance of 2020 pc, the motion of the nebula is equivalent to 102 km/sec.

Because the location of the geometric center is determined only within about 3″ in each direction and the location of the expansion center to within about 1″, all of these quantities are somewhat uncertain. This uncertainty amounts to 0.005″/yr for each component of the proper motion or more than 55 km/sec in the total motion and 40° in its orientation. Any discussion of the total space motion of the Crab Nebula must therefore be regarded with considerable skepticism.

An average radial velocity for the nebula can also be found if all the filaments are assumed to lie on the surface of a prolate spheroid located at a known distance. It must also be assumed that, in the reference frame of the nebula, each filament has its velocity proportional to its distance from the expansion center. As is pointed out above, this is only approximately true. Under these assumptions, the radial velocity of the

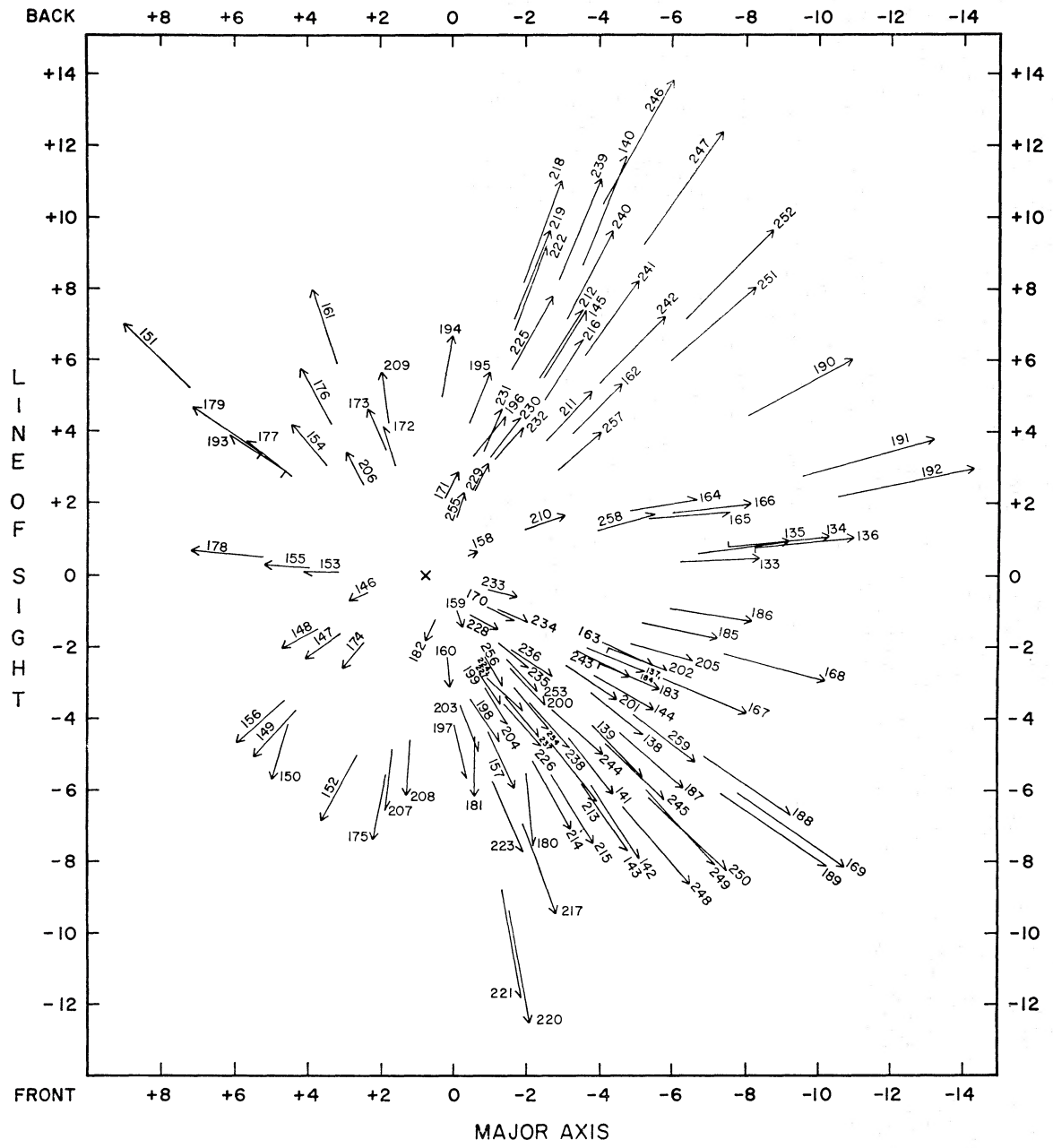

FIG. 3. 1950 positions and motions in 270 yr of the filaments of Table IV and Fig. 1 projected onto the plane through the major axis of the nebula and the line of sight. The scale is the same as in Plate I and Fig. 1, and X is the expansion center. The coordinates are in arbitrary units centered at the position of star D in the plane of the sky.

nebula is that V_R which makes

$$\sum_i (V_{r_i} - V_R) = \frac{4.74b}{\pi} \sum_i \frac{\mu_{x_i}}{x_i}\left[1 - \left(\frac{x_i}{a}\right)^2 - \left(\frac{y_i}{b}\right)^2\right] \quad (2)$$

and

$$\sum_i (V_{r_i} - V_R) = \frac{4.74b}{\pi} \sum_i \frac{\mu_{y_i}}{y_i}\left[1 - \left(\frac{x_i}{a}\right)^2 - \left(\frac{y_i}{b}\right)^2\right], \quad (3)$$

where the sum is taken over all the filaments; x and y are coordinates of a filament in seconds of arc along the major and minor axes of the ellipse in the plane of the sky; a and b are the semiaxes of that ellipse, 178″ and 120″, respectively; μ_x and μ_y are proper motions in (sec of arc)/yr along these axes; π is the assumed parallax (1/2020); and V_r is the radial velocity of a filament in km/sec. The velocity found by this method is −5.5 km/sec, confirming earlier statements (Baade; Woltjer) that the motion of the object is very nearly all in the plane of the sky.

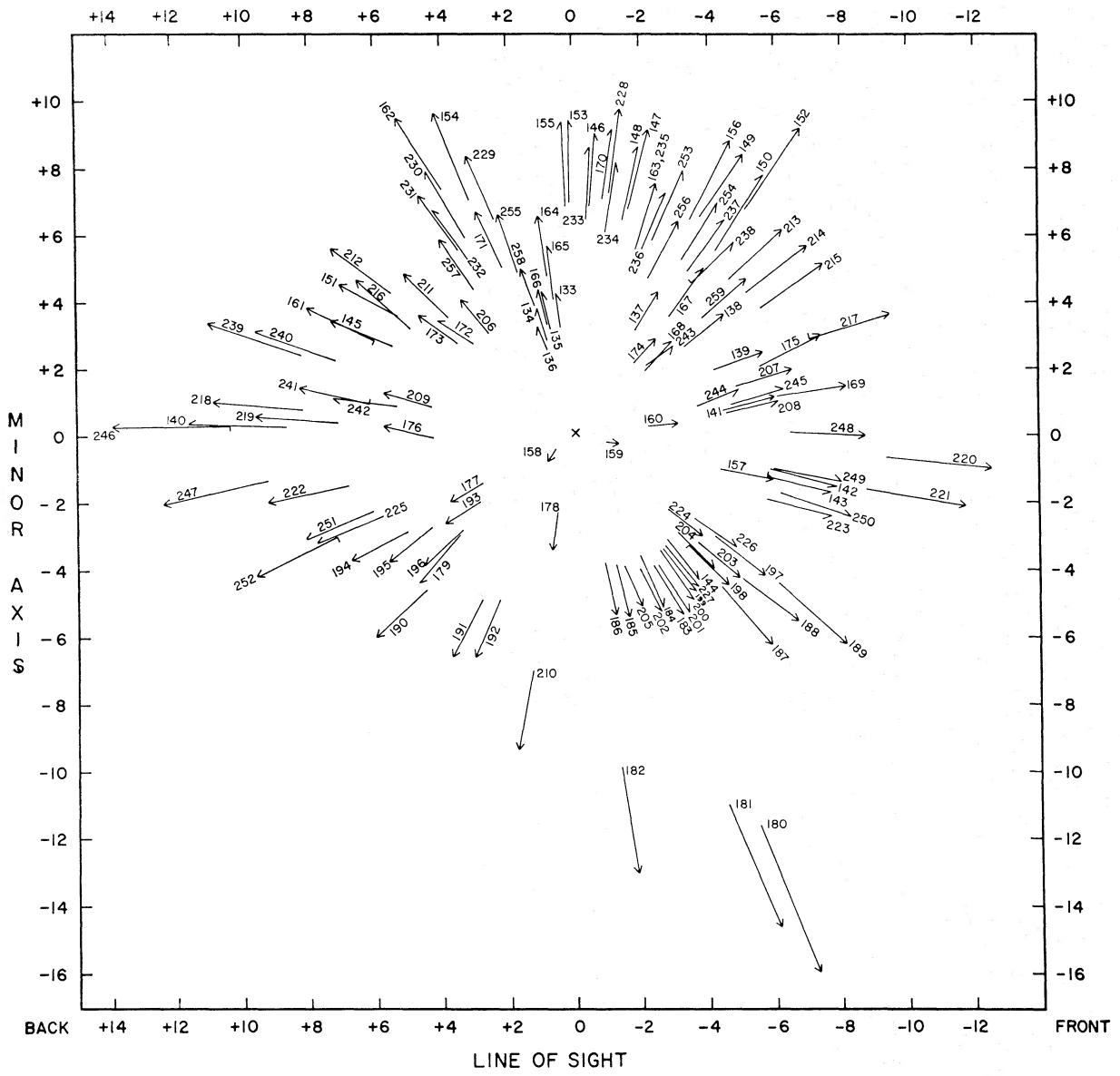

FIG. 4. 1950 positions and motions in 270 yr of the filaments of Table IV and Fig. 1 projected onto the plane through the minor axis and the line of sight. Scale and coordinates as in Fig. 3.

The motion of the nebula with respect to the galactic plane and the local standard of rest is then easily found by transforming to galactic coordinates ($l=184°$, $b=-6°$) and subtracting the basic solar motion [$\Pi=-9$ km/sec inward toward the galactic center; $\Theta=11$ km/sec faster than the circular velocity at the sun's position; and $Z=6$ km/sec upward from the plane of the galaxy (Delhaye 1965).] The resulting velocities are $\Pi=-11$ km/sec, $\Theta=+114$ km/sec, and $Z=+33$ km/sec.

A Population I object following a nearly circular orbit at the position of the Crab Nebula would have Π and Z near zero and Θ about -12 km/sec. This is just the difference of the circular velocities at the position of the sun (250 km/sec) and the nebula (238 km/sec; Schmidt 1965). A Population II object lagging behind the galactic rotation would have Θ still more negative. The Θ component found for the object is, therefore, improbable for either population type. The result is, however, extremely uncertain. The data are not inconsistent with Π and Z differing by 20 km/sec or so from the values given and a Θ as low as $+40$ km/sec.

The proper motion of the south preceding component of the central star, if converted to km/sec at a distance of 2020 pc, is equally improbable. The star's radial velocity is unknown, but it will in any case contribute almost exclusively to the Π component, leaving unchanged the $\Theta=+71$ km/sec and $Z=-86$ km/sec

found from proper motion alone. Each of these components is, however, uncertain by as much as 30 km/sec.

The difference between the relative proper motions discussed here and absolute proper motions is uncertain and may, in fact, be negligible. The effect will be, at most, a few percent of the motions of the individual filaments. The reduction to absolute proper motions is discussed by Trimble (1968).

If this unlikely pair of velocities is to be avoided, then either (a) the mass and geometrical centers of the nebula do not coincide and (b) the star in question is not associated with the nebula, or (c) a third, invisible fragment is carrying considerable momentum in the opposite, $-\Theta$, direction.

It has been suggested that this large space motion may be real and the Crab Nebula be a "runaway star" from the I Geminorum association. There are several reasons for doubting this. The direction of the nebular proper motion makes an angle of 80° with the direction in the plane of the sky from the center of the association to the nebula. The very small radial velocity found for the nebula is both improbable for an object shot out at random and inconsistent with the large difference in distance between the nebula (at 2.0 kpc) and the association (at 1.5 kpc). Finally, the mass contained in the filaments (Shklovskii 1966), as well as that of the star if it is a fairly ordinary sort of object at the distance of the nebula, is very much smaller than the masses of most runaways (Blaauw 1961).

IV. SUMMARY

Out of this maze of numbers several general conclusions emerge. First, the Crab Nebula is almost certainly located at a distance greater than 1.5 kpc, the balance of probability favoring something around 2 kpc.

Second, the line-emitting filaments are by no means confined to a thin ellipsoidal shell or envelope. For example (compare Plate I and Fig. 1 with the data in Table IV), the faint features numbered 158–160 and 218–225 are all closer than one-sixth of the minor axis to the center of the nebula in three as well as in two dimensions. In addition, three stronger features extend more or less radially out of the center. One of these, extending east-west on the east side of the nebula (filaments 161, 172–175, and 206–209), is a superposition of two regions of emitting material at the front and back of the object. A second dark feature, running north–south in the southern part of the nebula (filaments 176–179 and 193) is all on the far side of the object, while the third, running diagonally southeast to northwest toward the preceding edge of the nebula (filaments 183–187, 197–205, and 227) is entirely on the near side. These filaments might be thought of as extending somewhat radially within a thick shell. The adjacent features 194–196 are also close to the center of the object, but on the far side.

For the most part, the expansion is a radial one, each filament having a velocity approximately proportional to its distance from the expansion center. If this were not the case, the filaments would not converge to a single point at a single time in the past. The largest deviations from this rule of proportionality (300 km/sec and 0.032″/yr) are five or six times the probable error of the measurements and may be real. Some of these deviations occur in the "bulge" region, but there are a few in all areas of the nebula.

Since one-half of the filaments are within about 8″ of the expansion center at the date of best convergence (810 yr ago), the median deviation from radial expansion must be only about 0.010″/yr. There are not a sufficient number of data points available near the edges of the nebula to determine a similar quantity for the radial velocities, but the median deviation ought to be something like $4.74 \times 0.010 \times 2020/\sqrt{2}$ or 70 km/sec. These numbers are not significantly larger than the measuring errors, hence the deviations from purely radial expansion cannot be analyzed fruitfully.

The association of the nebula with the so-called central star is neither proved nor excluded, but, if true, it implies an extremely unusual space motion for both objects.

ACKNOWLEDGMENTS

The author is greatly indebted to Dr. Guido Münch, who originally suggested the project, has guided it throughout, and has taken plates especially for it. Thanks are also due to Dr. Jesse L. Greenstein, Dr. Richard P. Feynman, and Dr. Jan H. Oort, who read the manuscript and made many helpful suggestions, and to Dr. Rudolph Minkowski for the loan of observing charts and several illuminating conversations. Conversations with Dr. P. A. G. Scheuer, Dr. James E. Gunn, and Dr. Jeffrey D. Scargle were also most helpful.

APPENDIX: PROPER MOTIONS OF THE REFERENCE STARS

Table VI lists the coordinates x and y, proper motions μ_x and μ_y, and their standard deviations σ_x and σ_y, and approximate magnitudes for the 35 reference stars. The proper motions were determined by comparing each star with the remaining 34 for each of the five base lines 1939–1953, 1953–1966, 1939–1966 (100 in. plates), 1950–1964, and 1950–1966 (200 in. plates). The values tabulated are the means of the resulting five numbers.

Six of the stars (Numbers 5, 7, 8, 9, 23, and 29) have motions in the x and/or y directions which are larger than three times their standard deviations and are, therefore, probably real. One star has a relative proper motion of about 0.03″/yr. The others are all 0.02″/yr or smaller. Neither of the stars used in aligning the plates (A and B in Fig. 1, Nos. 1 and 2 in Table VI)

TABLE VI. Proper motions of the reference stars.

Star	m_{pg}	X	Y	μ_x ″/yr	σ_x ″/yr	μ_y ″/yr	σ_y ″/yr
1	16.5	+ 84″.3	− 6″.7	+.001	.001	−.001	.002
2	17.5	+170.3	+ 14.4	+.002	.003	+.005	.003
3	17.0	+ 75.3	+ 26.9	−.002	.001	−.005	.004
4	18.0	+ 97.0	+ 91.0	−.001	.002	+.003	.004
5	17.5	+ 79.4	+ 74.8	+.018	.001	−.019	.001
6	18.0	+ 19.5	+103.6	−.003	.002	−.004	.004
7	18.0	+ 15.9	+135.8	−.006	.001	−.005	.002
8	17.5	− 7.5	+109.2	−.005	.001	+.002	.003
9	18.0	− 49.3	+121.8	+.001	.003	+.007	.002
10	18.0	− 82.9	+114.2	−.006	.003	+.006	.004
11	18.0	−102.8	+120.9	−.002	.003	+.007	.004
12	18.0	− 96.9	+ 77.2	+.003	.001	−.007	.006
13	17.5	−164.8	+ 86.9	+.003	.005	+.006	.006
14	17.5	−148.2	+ 52.9	+.003	.005	−.001	.003
15	18.0	−153.7	+ 30.6	+.002	.005	−.002	.003
16	18.0	−107.4	+ 29.1	+.005	.007	+.004	.002
17	16.5	− 82.2	− 69.2	+.004	.004	−.018	.004
18	17.5	− 94.4	−105.6	−.000	.002	−.002	.004
19	18.0	− 61.9	−106.7	−.001	.004	−.002	.002
20	18.0	− 50.3	−118.3	+.002	.001	−.001	.002
21	17.5	+ 29.3	−106.1	−.004	.003	−.005	.002
22	17.5	+ 35.9	− 92.2	−.003	.002	−.001	.002
23	18.0	+ 62.7	− 99.4	−.004	.001	+.006	.001
24	18.0	+152.5	−128.8	−.002	.003	+.005	.007
25	17.5	+166.6	− 98.3	+.002	.005	+.011	.006
26	17.5	+101.3	− 37.5	+.001	.003	−.003	.003
27	17.0	+ 17.4	+ 2.7	+.003	.003	−.006	.003
28	16.0	0	0	−.001	.004	−.001	.007
29	16.0	− 2.5	− 4.2	−.009	.003	−.002	.003
30	17.0	− 0.6	− 14.7	−.001	.002	−.004	.002
31	18.0	− 2.0	− 16.7	−.004	.005	+.001	.004
32	15.5	+ 48.2	− 18.4	+.001	.002	−.009	.004
33	17.5	− 44.0	+ 53.1	+.000	.003	+.002	.004
34	16.0	− 52.9	+ 42.0	−.001	.004	+.004	.003
35	16.0	− 33.6	+ 59.8	−.002	.003	−.006	.003

has a detectable proper motion. Of the five stars near the center of the nebula (C through G of Plate I and Fig. 2, Nos. 27 to 31 in Table VI), only the south preceding component of the central double star has a motion that is likely to be real.

Magnitudes of the reference stars were estimated by visual comparison with stars of the north polar sequence and Selected Area 73 on plates taken by Baade with the 60 in. telescope diaphragmed down to a 40 in. diameter in order to reduce the disturbing effects of the nebulosity. The brightest stars were also compared with those stars in the vicinity of the Crab Nebula whose magnitudes are given by Orlova (1966). As can be seen from the table, this was done in an extremely approximate manner, since the magnitudes were intended for use only in estimating mean parallaxes.

REFERENCES

Baade, W. 1942, *Astrophys. J.* **96**, 109.
Binnendijk, L. 1943, *Bull. Astron. Inst. Neth.* **10**, 9.
Blaauw, A. 1961, *ibid.* **15**, 265.
Bowyer, S., Byram, E. T., Chubb, T. A., and Friedman, H. 1964, *Science* **146**, 912.
Brosche, P. 1966, *Z. Astrophys.* **64**, 1.
Delhaye, J. 1966, *Galactic Structure*, A. Blaauw and M. Schmidt, Eds. (University of Chicago Press, Chicago), p. 74.
Deutsch, A. N., and Lavdovsky, V. V. 1940, *Poulkovo Obs. Circ.* **30**, 21.
Duncan, J. C. 1939, *Astrophys. J.* **89**, 482.
Duyvendak, J. J. L. 1942, *Publ. Astron. Soc. Pacific* **54**, 91.
Gower, J. F. R. 1967, *Nature* **213**, 1213.
Greenstein, J. L., and Trimble, V. L. 1967, *Astrophys. J.* **149**, 283.
Kamp, P. van de 1941, *Ann. New York Acad. Sci.* **42**, 151.
——. 1962, *Astronomical Techniques*, W. A. Hiltner, Ed. (University of Chicago Press, Chicago), p. 487.
Kraft, R. P. 1967 (private communication).
Maanen, A. van 1928, *Mt. Wilson Contrib.* No. 356.
Matveenko, L. I., and Sorochenko, R. L. 1968, *Soviet Astron.—A. J.* **11**, 557.
Minkowski, R. 1942a, *Astrophys. J.* **96**, 306.
——. 1942b, *ibid.* **96**, 121.
Minkowski, R. 1964, *Annual Review of Astronomy and Astrophysics*, L. Goldberg, A. Deutsch, and D. Layzer, Eds. (Annual Reviews, Inc., Palo Alto, California), Vol. 2, p. 247.
——. 1966, *Astron. J.* **71**, 371.
Münch, G. 1958, *Rev. Mod. Phys.* **30**, 1042.
Oda, M., Bradt, H., Garmire, G., Spada, G., Sreekantan, B. V., Gursky, H., Giacconi, R., Gorenstein, P., and Waters, J. R. 1967, *Astrophys. J.* **148**, L5.
Orlova, O. N. 1966, *Publ. Astr. Obs. Pulkova* **24**, 115.
Scargle, J. 1968, thesis, California Institute of Technology.
Schmidt, M. 1966, *Galactic Structure*, A. Blaauw and M. Schmidt, Eds. (University of Chicago Press, Chicago), p. 528.
Shklovskii, I. S. 1966, *Soviet Astron.—A. J.* **10**, 6.
Trimble, V. L. 1968, thesis, California Institute of Technology.
Woltjer, L. 1958, *Bull. Astron. Inst. Neth.* **14**, 39.

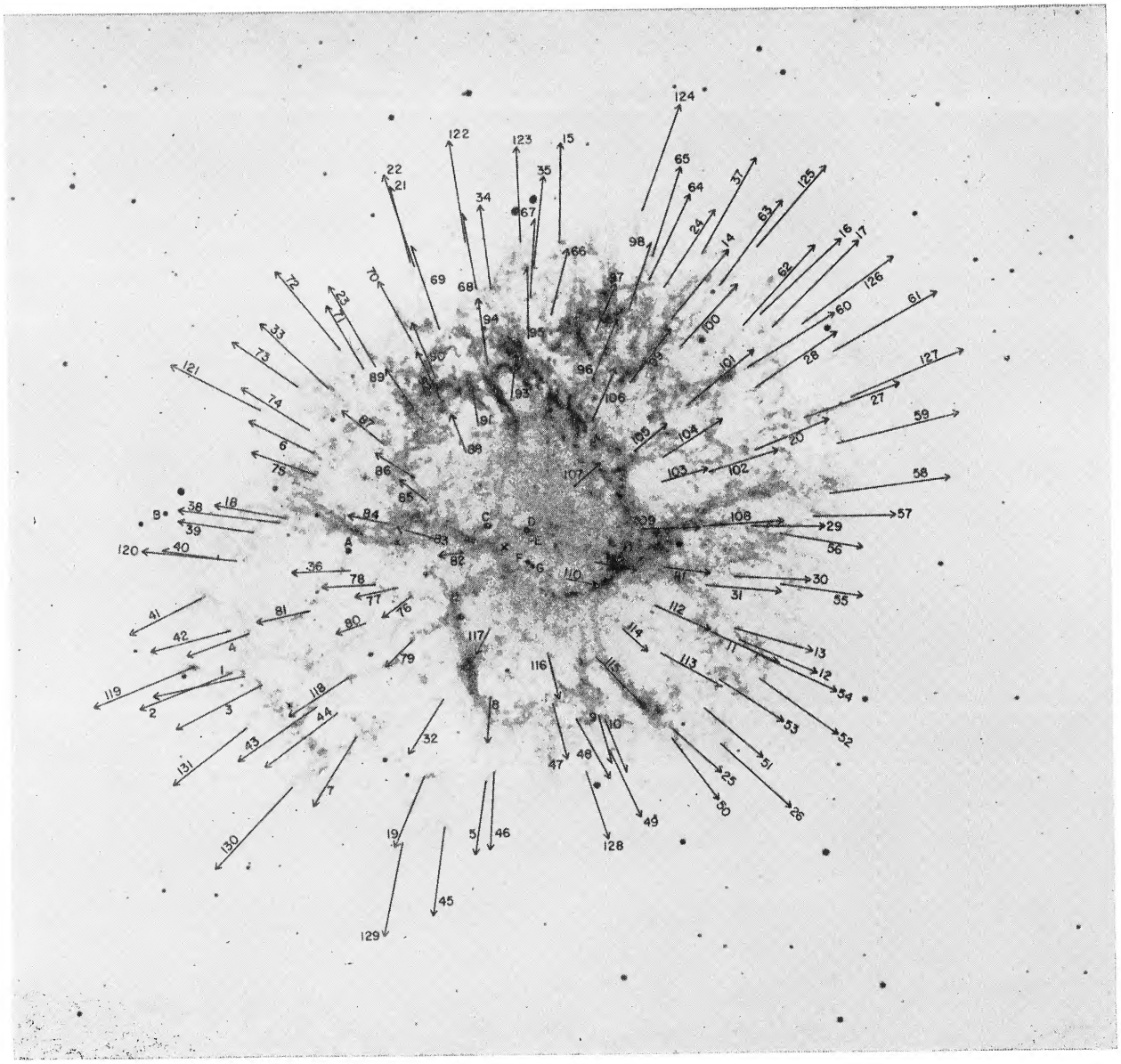

PLATE I (No. 1, Trimble). Proper motions for 132 positions in the Crab Nebula as listed in Table II. The arrows represent the distance the filaments will move in about 270 yr at their present rates. The center of the expansion is located at the point marked X. The stars used to align the plates for measurement and those nearest the center of the nebula are lettered. The photograph was taken through an Hα interference filter on the 200-in. telescope by Münch.

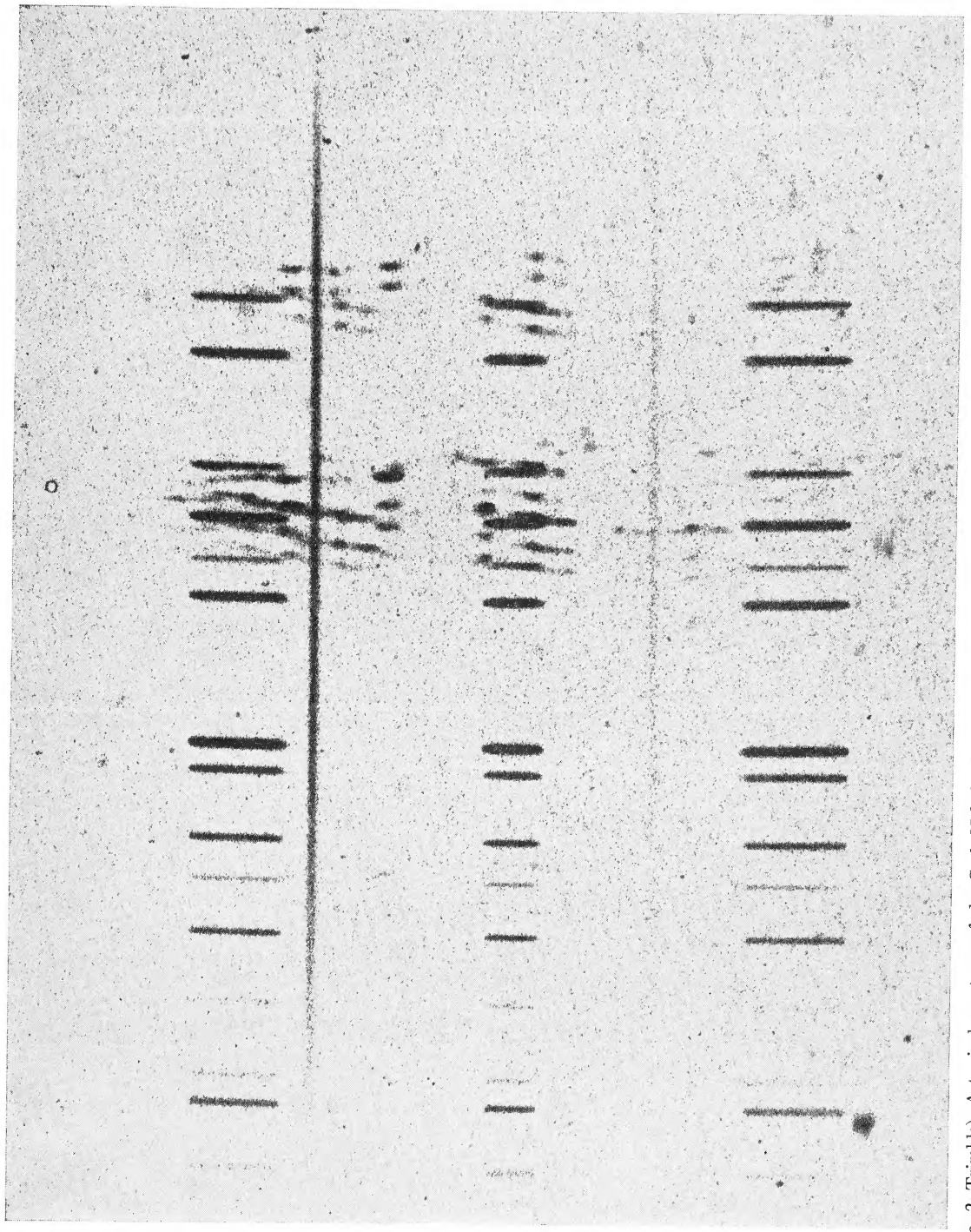

PLATE II (No. 2, Trimble). A typical spectrum of the Crab Nebula showing about 30 separate measurable features (some of which have been lost in the reproduction process). The two streaks perpendicular to the slit direction are stars separated by about 1.5 in the plane of the sky. The lines of two or more features may be partially blended as, for example, at the points marked *X*.